Tutor/s

Dr. Jordi Ignés-Mullol
Departament de Ciència de Materials i Química Física

Dr. Carlos Rodríguez-Abreu
Dr. Santiago Grijalvo Torrijo
IQAC-CSIC
CIBER BBN

Grau de Química

Treball Final de Grau

Preparation of Ternary Non-Viral Vectors for Central Nervous System Disorders.

Preparació de Vectors No Virals Ternaris per als Transtorns del Sistema Nerviós Central.

Víctor Espinosa Gómez

March 2022

ciber-bbn
Biomedical Research Networking Center
Bioengineering, Biomaterials, Nanomedicine

Universitat de Barcelona

BKC Barcelona Knowledge Campus
Campus d'Excel·lència Internacional

“We build too many walls and not enough bridges”

Sir Isaac Newton

Me gustaría agradecer a los grupos QCI y CIBBER del CSIC por la oportunidad que me han dado al dejarme trabajar con ellos y, sobre todo, al Dr. Santiago Grijalvo por guiarme y por toda la ayuda que me ha dado durante estos meses. Gracias a mis padres y a mi familia por acompañarme y apoyarme todos estos años. Gracias a todos los profesores y compañeros que han estado ahí todos estos años del grado ayudándome a seguir aprendiendo y avanzando.

REPORT

CONTENTS

1. SUMMARY

The use of nanosystems for the treatment of brain disorders, like cancer, has emerged in recent years. In this project, a ternary system based on poly(lactic-co-glycolic acid) (PLGA), chitosan and 2'-deoxy-5-fluorouridine (FdU) has been engineered as a promising non-viral vehicle in which all the components interact via electrostatic forces. The goal is to find a strategy to transport FdU, which acts as a therapeutic molecule. We hypothesised that our system, owing to its nanometric properties, might go through the blood-brain barrier (BBB). A formulation composition in which the nanosystem is stable has been found, exhibiting a small diameter, low polydispersity index values and a positive ζ-potential. We demonstrated that tumour cells were able to take up our nanosystem, according to flow cytometry analyses. In addition, MTT assays indicate that the nanosystem displays certain degree of toxicity in cancer cells. *Trans*-Ferulic acid (FA) was encapsulated in PLGA NPs and 50% of the drug was released gradually after 9 hours.

Keywords: Blood-brain barrier, Drug delivery, Nanomedicine, Nanoparticles, Neurodegenerative disease, PLGA

2. RESUM

L'ús de nanosistemes per tractament de trastorns cerebrals, tals com el càncer, s'ha estès en els darrers anys. En aquest projecte s'ha dissenyat un sistema ternari no viral basat en poly(lactic-co-glycolic acid) (PLGA), quitosà i 2'-deoxy-5-fluorouridine (FdU) que s'uneix entre si degut a forces electroestàtiques. La finalitat és trobar una estratègia per transportar FdU, que actua com molècula terapèutica. Suposem que el nostre sistema, degut a les seves característiques nanomètriques, podria travessar la barrera hematoencefàlica. S'ha trobat una relació molar de cada un dels seus components on el nanosistema es estable, exhibeix un diàmetre de partícula petit, l'índex de polidispersitat és baix i el ζ-potencial és positiu. Hem comprovat que cèl·lules tumorals capten el nanosistema, segons anàlisi de citometria. A més, té una certa toxicitat en cèl·lules cancerígenes que s'ha estudiat en assaigs MTT. Àcid *trans*-ferulic (FA) es va encapsular en nanopartícules de PLGA i un 50% de la droga es va alliberar gradualment després de 9 hores.

Paraules clau: Barrera hematoencefèlica, Alliberació de fàrmacs, Nanomedicina, Nanopartícules, Malalties neurodegeneratives, PLGA

3. INTRODUCTION

3.1. TUMOURS OF THE CENTRAL NERVOUS SYSTEM (CNS): CLASSIC THERAPIES AND STRATEGIES

The brain is isolated from the blood by the blood-brain barrier (BBB), an endothelial barrier, which prevents the entry of drugs and other substances from the blood to the CNS (Fig. 1) [1]. Brain tumours can be divided into primary and metastatic tumours. The first ones emerge from the brain, while metastatic tumours arise elsewhere in the body [2]. While it is known that ionizing irradiation on the cranium may increase the incidence of brain tumours, there is little information about the relation of other environmental factors to primary brain tumours [3].

Classical strategies for the treatment of brain tumours are surgery, radiation therapy and chemotherapy. Surgery is helpful to remove the entire tumour localized in a specific region. Radiation treatments can be performed to kill residual tumour cells. Chemotherapy can be used either as primary therapy or in combination with both surgery and radiation therapies [4].

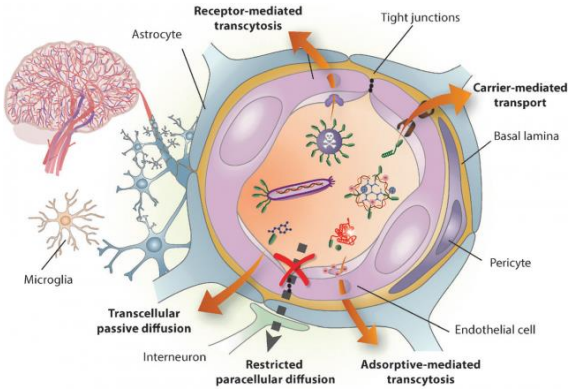

Fig. 1. Blood-brain barrier drawing. *(Image taken from ref. 26)*

3.2. NANOMEDICINE: NEW STRATEGIES

New therapeutic strategies have emerged with the aim to solve the limitations of classic treatments. BBB restrictions are the main limitation that novel therapies have to face. Nowadays, the use of nanotechnology has become an attractive strategy to treat cancer and other disorders through nanomaterials made up of biocompatible polymers, lipids, or dendrimers, among others that are complexed or conjugated with anticancer drugs (Fig. 2). These nanomaterials are

expected to bypass the BBB and therefore provide high concentrations of therapeutic agents at the target site [5].

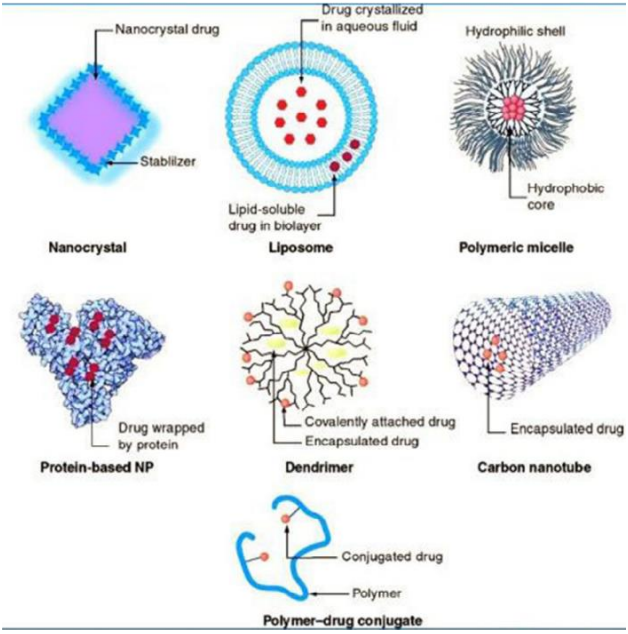

Fig. 2. Drug delivery system based on nanomaterials: nanocrystal, liposome, polymeric micelle, protein-based NPs, dendrimer, carbon nanotube and polymer-drug conjugate. (*Image taken from ref. 27)*

3.3. THE PROPOSED TERNARY SYSTEM

In this project, we present a new strategy for brain cancer therapies. It consists of a novel ternary system based on polymeric nanoparticles. As displayed in figure 3, the main core of this system is poly(lactic-co-glycolic acid) (PLGA), a synthetic polymer, which is covered and decorated first with chitosan (CH) and 5-fluorodeoxyuridine (FdU) to build up the expected three-layered system. It is expected that the resultant nanosystem is small enough to be permeable to the BBB.

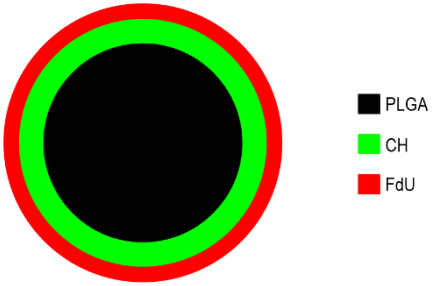

Fig. 3. Representation of the ternary system made up of PLGA (Black color), chitosan (green color), and FdU (red color).

3.3.1. Poly(lactic-co-glycolic acid) and its properties

Poly(lactic-co-glycolic acid) (PLGA) is a synthetic polymer that has been widely used in past studies owing to their biodegradable, biocompatible, and non-toxic properties [6]. PLGA polymer tends to be hydrolysed in two monomers, i.e., lactic acid and glycolic acid, which are later metabolized by the Krebs Cycle (Fig. 4). This is the reason why PLGA is considered a biodegradable and biocompatible polymer [7].

PLGA has various applications in drug delivery [6], tissue engineering [8] and medical devices. This work focuses on the use of PLGA NPs as a drug delivery system as a treatment for CNS disorders.

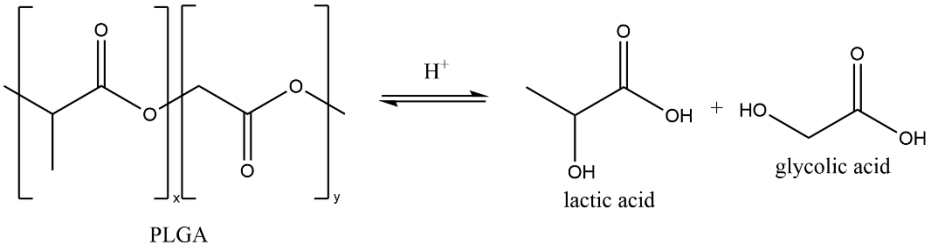

Fig. 4. Hydrolysis of PLGA leading to lactic acid and glycolic acid.

PLGA NPs can be easily prepared via nano-emulsions. Nano-emulsions are one type of emulsions containing nano-size droplets. Usually, their size ranges may vary from 50 to 200 nm. Nano-emulsions are typically transparent or translucent, though they can lose that transparency over time. They are not thermodynamically stable, even if they are kinetically stable [9,10]. Due to their small sizes, nano-emulsions undergo the Ostwald ripening mechanism which is the

principal process of their destabilisation [10]. Ostwald ripening is a process where one droplet increases its size at the expense of smaller ones thus the result is raising the average size of the nano-emulsion [11].

There are several methods for the preparation of nano-emulsions. These are mainly, divided into high-energy emulsification methods and low-energy emulsification methods [12]. There are also different low-energy methods: Phase inversion temperature (PIT) and phase inversion composition (PIC) methods. In the PIT method, changes in temperature affect the surfactant spontaneous curvature as shown in figure 5A (obviously, this method can only be applied to surfactants sensitive to temperature). In the PIC method, phase transitions are induced by changes in the composition at a constant temperature, as shown in figure 5B [12, 13]. In this project, nano-emulsions will be prepared via the PIC method.

PLGA NPs are able to encapsulate different types of hydrophobic drugs and can internalize cells and release drugs. After releasing the drug, PLGA is hydrolysed and metabolised, as shown above.

Surface charge is one important factor, positive-charged particles internalize more easily but can escape after the internalization. PLGA NPs have a negatively charged surface, but there are different methods to modify the surface and shift the charge [7]. Surface charge is measured by ζ-potential analysis. Modifications of the surface have also other purposes, such as targeting the organ to increase selectivity.

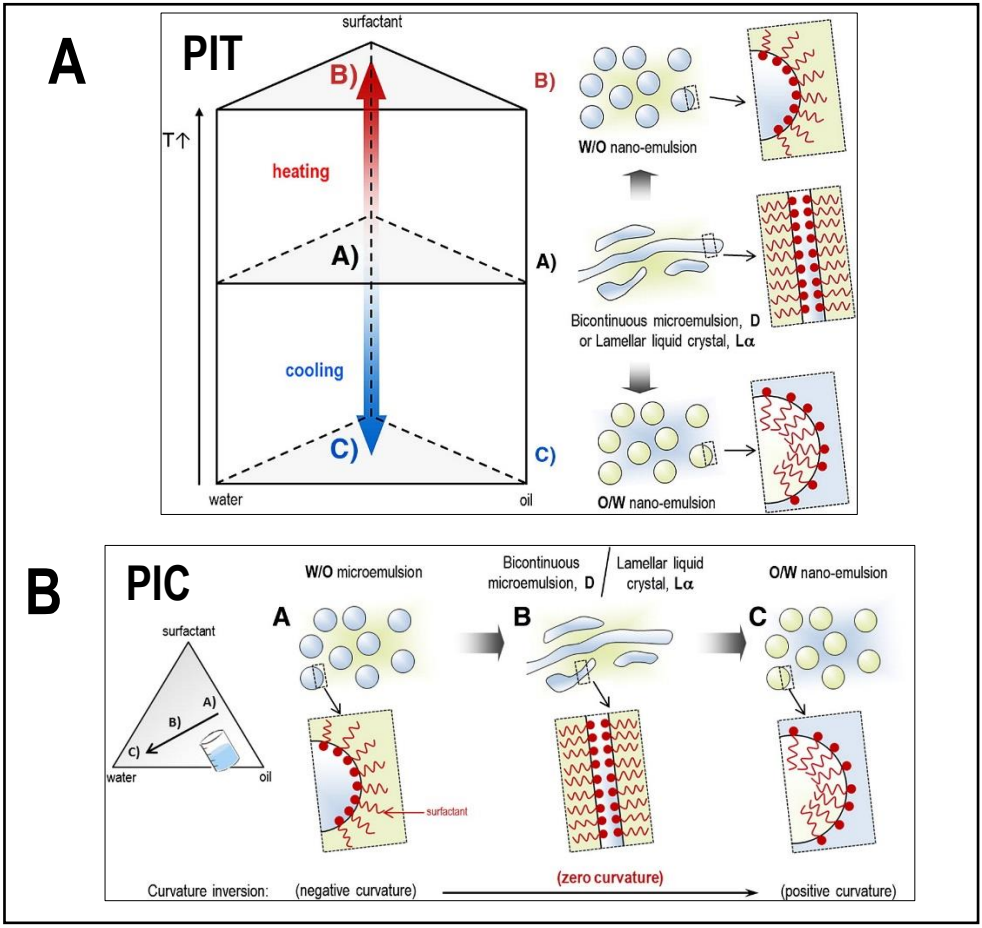

Fig. 5. A – Schematic representation of the formation of nano-emulsions by the PIT method. B – Schematic representation of the formation of nano-emulsions by the PIC method. *(Image adapted from ref. 12)*

3.3.2. Chitosan as a coating

Chitosan is a polysaccharide; its surface charge is positive (Fig. 6). It is biodegradable, biocompatible, and non-toxic [14,15]. It has many uses in biomedicine as drug delivery systems, dressings, and tissue engineering scaffolds among many others [14, 15, 16].

Chitosan is used as a surface coating for PLGA NPs. Thanks to its positive charge, it is possible to shift the charge of NPs from negative to positive using layer-by-layer (LbL) techniques.

There are different ways to incorporate chitosan into PLGA NPs, including the use of crosslinkers or during the emulsification in the preparation of PLGA [17].

As chitosan exhibits a positive surface charge, it will form an electrostatic, non-covalent bond with negatively-charged PLGA NPs.

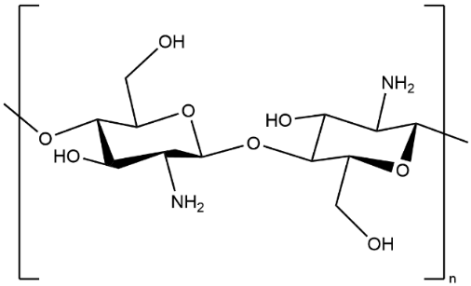

Fig. 6. Structure of Chitosan.

3.3.3. 5-fluorodeoxyuridine (FdU)

FdU is a pyrimidine analogue, a deoxyriboside derivative of 5-FU (Fig. 7). Thanks to its antitumoral activities, both FdU and 5-FU have been involved in cancer therapies for the treatment different tumours. FdU requires cellular uptake to prompt cytotoxicity. It enters cells through facilitated nucleoside transport systems [18].

The cytotoxicity effects are induced by inhibition of DNA synthesis via FdU inhibition of thymidylate synthase (TS). FdU inhibits TS, which causes an imbalance and causes cell death [19]. A study by Eidinoff in 1959 showed that cells exposed to FdU for 30 minutes were unable to grow when incubated in DMEM after removing the FdU [20].

FdU is the last piece of the ternary system this project proposes. FdU, having a negative surface charge, forms an attractive electrostatic bond with the chitosan layer covering in turn the PLGA layer.

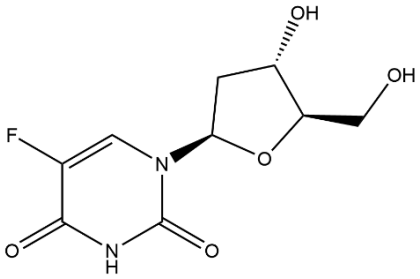

Fig. 7. Structure of 5-fluorodeoxyuridine.

3.4. CHARACTERIZATION TECHNIQUES

The most influential factors in the preparation of NPs are their size and surface charge. These elements affect the fate of NPs have on cells, including cellular uptake, toxicity and drug release at specific target sites [21]. Because of that, the most common techniques to measure particle size and surface charge are briefly explained below.

3.4.1. Dynamic Light Scattering

Dynamic Light scattering (DLS) is a non-destructive, non-invasive technique used to study the properties of different types of solutions and suspensions, including polymers and macromolecules. One of its purposes is to determine the size of particles.

DLS measures time-dependant fluctuations in the scattering intensity originating from particles undergoing random Brownian motion. These fluctuations can provide information on the diffusion coefficient and size of particles [22].

3.4.2. ζ-Potential

Systems submerged in an aqueous liquid are prone to develop a surface charge. A consequence of this is that contra-ions can build up on the surface. The distribution of the different charges on the surface establishes the potential.

The particle's movement sweeps along with the solvent and the contra-ions up to a distance equivalent to the solvation radius. The ζ-potential of the particle is determined by the combination of its charge plus the charge that is dragging. A colloid with a ζ-potential equal to zero will tend to aggregate. ζ-Potential might be influenced by pH, ionic strength, and concentration, being pH the most influential [21].

3.4.3. Dark-Field microscopy

Dark-Field microscopy is an effective technique for imaging samples that are not well imaged in normal illumination conditions. In order to create the contrast of the dark background characteristic of dark-field microscopy, the light source is blocked only allowing oblique rays to pass through the specimen. The light that reaches the sample is diffracted, reflected, and refracted into the microscope objective.

Dark-Field microscopy has a lot of applications in biological and metallurgical sciences and is especially useful for suspensions, liquid substances, and characterization of nanomaterials.

4. OBJECTIVES

The main objectives of this work are the synthesis and characterization of unloaded and drug-loaded PLGA NPs, the preparation and characterization of positively charged ternary systems PLGA-chitosan-FdU, the study of their biological viability and determining the release rate of a model drug (Ferulic acid).

5. EXPERIMENTAL SECTION

5.1. MATERIALS AND METHODS

All solvents and chemical reagents were of reagent grade and used as received. 5-fluorodeoxyuridine (5-FdU) was kindly provided by Ramon Eritja's research group (IQAC, CSIC). Poly(lactic-*co*-glycolic acid) (PLGA) from Boheringer Ingelheim (Ingelheim am Rhein, Germany.) was used for the preparation of NPs. Phosphate buffered saline (PBS; pH 7.2 - 7.6) was freshly prepared from phosphate buffered saline tablets (Merck, Sant Louis, MO, USA). Chitosan (CH; low molecular weight 50,000 - 190,000 Da) and Coumarin-6 (Cou) were purchased from Merck (Sant Louis, MO, USA). Acetonitrile (>99%; HPLC Grade) was purchased from Fisher Scientific (Waltham, MA, USA). Acetic acid (96%) and glacial acetic acid (>99%) were purchased from Merck (Sant Louis, MO, USA) and Panreac (Barcelona, Spain), respectively. Ethanol (absolute) and Potassium dihydrogen phosphate (KH_2PO_4) were purchased from Merck (Sant Louis, MO, USA). Ethyl acetate (99.5%) was purchased from Panreac (Barcelona, Spain). Dimethyl sulfoxide (DMSO), Polysorbate 80 (Tween 80) and trans-ferulic Acid (FA) (>99%) were purchased from Merck (Sant Louis, MO, USA).

5.2. UNLOADED PLGA NPS PREPARATION

PLGA NPs were prepared via single-emulsion evaporation method. The emulsion consists of a water phase, an organic phase, and a surfactant. The aqueous phase covers 90% of the total,

while the organic phase represents 7 wt% (containing 4 wt% of PLGA). The surfactant constitutes the remaining 3 wt%.

11.2 mg of PLGA were dissolved in 140 µL of ethyl acetate. 120 µL of Tween 80 were dissolved in 140 µL of ethyl acetate with help of a vortex to homogenize. The two solutions were mixed, and 3.6 mL of PBS were added dropwise with a constant vortex to form the O/W nano-emulsion. To evaporate the solvent, rotary evaporation was performed for one hour at 25 ºC and 155 rpm and 43 mbar. The amount of Milli-Q water needed to reach 4 mL was added afterwards.

5.3. Loaded PLGA NPs Preparation

The protocol to prepare loaded PLGA NPs is similar to the unloaded protocol described above. In this case, an appropriate amount of the drug is dissolved in ethyl acetate together with the PLGA polymer in order to facilitate drug entrapment within the polymeric network. Some quantities are modified to maintain the final volume.

5.3.1. Cou-loaded NPs

A stock solution of 2 mg/mL of Coumarin-6 (Cou) in ethyl acetate was prepared. 20 µL of the aforementioned solution was added to a solution of 11.2 mg of PLGA dissolved in 130 µL of ethyl acetate. Tween 80 was dissolved in 130 µL of ethyl acetate. 3.6 mL of PBS was added dropwise with constant vortex. Rotary evaporation was performed for one hour. The amount of Milli-Q water needed to reach 4 mL was added afterwards, as described above.

5.3.2. FA-loaded NPs

A stock solution of 4 mg/mL of trans-ferulic Acid (FA) in ethyl acetate was prepared. 50 µL of the stock solution was added to a solution of 11.2 mg of PLGA dissolved in 115 µL of ethyl acetate. Tween-80 was dissolved in 115 µL of ethyl acetate. 3.6 mL of PBS was added dropwise with constant vortex. Rotary evaporation was performed for one hour and an amount of Milli-Q water needed to reach 4 mL was added afterwards.

5.4. Synthesis of the Ternary System

A 1 mg/mL solution of chitosan in 1% acetic acid was prepared. FdU was diluted in Milli-Q water to obtain a 3.94×10^{-6} mol/L solution.

Firstly, the binary system was prepared by mixing 480 µL of the chitosan solution with 515 µL of the FdU solution. The mixture was stirred and left to incubate at room temperature for 30 minutes. After that time, the ternary system was prepared by mixing 336 µL of PLGA NPs (loaded or unloaded) and 15 µL of Milli-Q water with the binary system and then stirred and left for 1 hour at room temperature to promote complexation with PLGA (Table 1).

Molar ratio (PLGA:CH:FdU)	CH (µL)	FdU (µL)	PLGA (µL)	Milli-Q water (µL)	Total (µL)
46:2:1	480	515	336	15	1346

Table 1. Used volumes for the preparation of the ternary system.

5.5. PHYSICOCHEMICAL CHARACTERIZATION

The mean size of NPs was analysed with a 3D-DLS dynamic light scattering instrument (LS Instruments AG., Freiburg, Switzerland) equipped with He-Ne laser (λ = 632.8 nm) and detection range from 0.5 nm to 5 µm. Measurements were carried out in triplicate at a scattering angle of 90º and a temperature of 25 ºC. The viscosity of the medium was taken as 0.937 cP. The refractive index of PBS was 1.334 as determined on an Abbe refractometer (Atago 3 T, Japan) at 25 ºC. DLS data were treated by cumulant analysis to obtain the hydrodynamic diameter and polydispersity index (PDI).

Zeta potential was determined from the electrophoretic mobility measured by laser Doppler velocimetry using ZetaSizer Nano ZS laser diffractometer (Malvern Instruments, UK) applying the Smoluchowski equation (eqn. 1). For the measurements, nanoparticle dispersions were diluted with distilled water. Each sample was measured in triplicate at 25 ºC.

$$\mu = \frac{\varepsilon \varepsilon_0}{\eta} \qquad \text{eqn. 1}$$

Kinetic stability of the NPs was obtained using a Turbsican Lab backscattering stability analyser (Formulaction). Stabilities were performed in triplicate at 37 ºC for 24h.

The ternary system was characterised by means of hyperspectral imagining and mapping of each compound by using optical microscope with enhanced dark field (Cytoviva, Auburn, AL, USA).

5.6. *IN VITRO* RELEASE ASSAY

Firstly, FA was encapsulated in PLGA NPs at a concentration of 0.05 mg/mL, following the experimental protocol described in section 5.3. Secondly, a dialysis bag (MWCO >3,500 Da) was

soaked in PBS for 10 minutes. 1 mL of drug loaded PLGA NPs were added to the dialysis bag. The bag was left suspended in 40 mL of PBS or PBS/Ethanol (15% of ethanol) at 37 ºC. After predetermined times, 1 mL of PBS was taken and replaced with 1 mL of fresh PBS.

The cumulative release was monitored using a HPLC instrument with an UV lamp using ACH/H_2O as mobile phase.

As a control, the release for FA was performed using FA at the same concentration but without being encapsulated. In this case, the receptor phase was PBS/Ethanol (15% ethanol).

5.6.1. Mathematical models

Release curves were fitted according to First order (eqn. 2), Higuchi (eqn. 3), Korsmeyer–Peppas (eqn. 4) and Hixson-Crowell (eqn. 5) empirical equations. In the First order model, Q_o is the initial concentration of drug, K is first order constant, and t is time. In the Higuchi model, k is a constant related to the formulation, and M_t and M_∞ are the cumulative and the maximal amount of drug released at time t, respectively. In the Korsmeyer-Peppas model, k is a rate constant, n is the diffusion coefficient that characterizes the release mechanism. n = 0.5 for Fickian diffusions and 0.5 < n < 1 for non-Fickian diffusions. In the Hixson-Crowell model, W_o is the initial amount of drug, W_t is the remaining amount of drug at time t, and κ is a constant that incorporates surface-volume relation.

$$logQ_t = logQ_o + \frac{Kt}{2.303} \quad \text{eqn. 2.}$$

$$\frac{M_t}{M_\infty} = k\sqrt{t} \quad \text{eqn. 3.}$$

$$\frac{M_t}{M_\infty} = kt^n \quad \text{eqn. 4.}$$

$$W_o^{1/3} - W_t^{1/3} = \kappa t \quad \text{eqn. 5.}$$

5.7. *IN VITRO* CELL CULTURE EXPERIMENTS

Two *in vitro* cell culture experiments were carried out: (1) Cytotoxicity, which was evaluated using the MTT assay and (2) cellular internalization which was evaluated by flow cytometry. HeLa cells were cultivated in DMEM at 37 ºC and 5% CO_2 atmosphere.

5.7.1. Colorimetric MTT assay

MTT assay was performed as described by Mosmann [23] with some modifications.

Roughly 5,000 cells were added to each well of a 96-well plate along with 300 µL of medium and incubated for 24 hours. The medium was replaced with 100 µL of medium containing different concentrations of the ternary system and incubated for another 24 hours (Table 2). The NP-containing media was then removed and replaced with 100 µL of DMEM. After another 24 hours of incubation time, 10 µL of MTT were added, and cells were incubated for 3 hours approximately. Finally, 200 µL of DMSO was added to dissolve formazan crystals. MTT absorbance was measured at 570 nm.

[PLGA] (mg/mL)	Ternary System (µL)	DMEM (µL)	Total volume (µL)
0.03	4.29	95.71	100.00
0.04	5.72	94.28	100.00
0.05	7.15	92.85	100.00
0.06	8.58	91.42	100.00

Table 2. Used volumes of PLGA:CH:FdU and DMEM for the MTT assay.

5.7.2. Cellular Uptake

Cytometry is a fluorescent technique, so a fluorescent compound is needed in the study.

Cou-loaded PLGA NPs were synthesised just before doing the assay. The system used in the cellular uptake study did not contain FdU, as the intention is to measure the number of particles that are able to internalise within cells.

A 24-well plate was used, in which two concentrations of PLGA NPs were tested (Table 3). With a total volume of 300 µL for each well, they were filled with the amount of NPs needed to obtain the desired concentration; the rest was DMEM (Table 3). After 24 h in the incubator at 37 ºC and 5% CO_2 atmosphere, cells were trypsinised, centrifuged and re-suspended in PBS. The amount of fluorescently labelled cells was then measured in a cytometer.

[PLGA] (mg/mL)	Binary System (µL)	DMEM (µL)	Total volume (µL)
0.221	94.85	205.15	300.00
0.110	47.21	252.79	300.00

Table 3. Used volumes of PLGA:CH in relation to PLGA concentration for cellular uptake test.

6. RESULTS AND DISCUSSION

6.1. PHYSICOCHEMICAL CHARACTERIZATION

Many attempts were carried out during the optimisation of the protocol for the ternary system. We used different PLGA:Chitosan molar rations in order to promote the formation of the first layer. Two strategies were investigated: (1) Mixing CH and PLGA at appropriate molar ratios and centrifugation of the binary system (PLGA:CH) [24, 25]. Unfortunately, this strategy produced particle aggregation, hence large sizes and high polydispersity values were obtained. (2) The second strategy, relied on the preparation of the CH:FdU binary system, and subsequent incorporation of PLGA NPs which were added to complete the ternary system as explained in section 5.4. The optimisation was carried out at different PLGA - CH - FdU molar ratios.

6.1.1. ζ-Potential

All synthetized NPs were characterized in terms of ζ-Potential. Modification of CH:FdU in PLGA NPs shifted the surface charge from negative to positive (Table 4). Molar ratios of 5:1:1 (PLGA:CH:FdU) were measured, but we observed that these selected relations displayed a ζ-potential much more positive than intended (entries 2-4). These positive values might result toxic in cell culture studies. Therefore, we tried to reduce the net positive charge value by adding higher PLGA concentrations (entries 5-7) (Table 4). These molar ratios were selected and characterised in terms of dynamic light scattering.

Entry		ζ-Pot (mV)	Size (nm)	PDI
1	PLGA NPs	-24.53 ± 0.51	34.93 ± 1.52	0.37 ± 0.01
2	PLGA:CH:FdU (5:1:1)	43.5 ± 2.19	-	-
3	PLGA:CH:FdU (5:1.5:1)	37.2 ± 0.636	-	-
4	PLGA:CH:FdU (5:2:1)	40.5 ± 1.34	-	-
5	PLGA:CH:FdU (46:1:1)	15.5 ± 0.456	54.1 ± 9.5	1.11 ± 0.24
6	PLGA:CH:FdU (46:1.5:1)	11.9 ± 2.20	85.4 ± 6.1	0.67 ± 0.06
7	PLGA:CH:FdU (46:2:1)	24.1 ± 2.56	57.46 ± 1.24	0.45 ± 0.05
8	PLGA:CH:FdU (46:2.5:1)	-	61.52 ± 1.17	1.27 ± 0.13
9	PLGA:CH:FdU (50:2.5:1)	-	53.78 ± 2.85	1.33 ± 0.78

Table 4. ζ-Potential, particle size and PDI of PLGA NPs and the ternary system at different molar ratios of each component.

6.1.2. Particle Size

The hydrodynamic diameter and PDI values were measured using DLS. As expected, PLGA:CH:FdU showed a larger diameter than non-coated PLGA NPs (Table 4). The PDI of the ternary system differed for different molar ratios of its components. Unexpectedly, we observed PDI values greater than 0.5 (high polydispersity) when both the CH and PLGA molar ratios increased (1.11, 0.67, 1.27 and 1.33 for ratios PLGA:CH:FdU 46:1:1; 46:1.5:1; 46:2.5:1; 50:2.5;1, respectively). Interestingly, the PLGA:CH:FdU molar ratio 46:2:1 displayed a lower PDI and small hydrodynamic diameter (Table 4, entries 5-9). We suspect that the system 46:2:1 had a surface charge sufficiently positive to exhibit compaction that lowers both size and PDI values (Table 4, entry 7). Further assays were carried out with the system at 46:2:1 molar ratio.

6.1.3. Turbiscan Stability Test

As mentioned in section 3.3.1, nano-emulsions are not thermodynamically stable. Turbiscan stability analyser can detect two types of destabilization via BackScattering (BS) and Transmission (T) measurements: (1) Particle size variation: Ostwald ripening and aggregation, and (2) Physical stability: sedimentation and creaming. Figures 8A and 8B shows ΔT and ΔBS profiles, respectively, of PLGA:CH:FdU (46:2:1) particles. The lack of peaks associated to creaming (negative peak corresponding to the upper part of the vial) and sedimentation (positive peak corresponding to lower part of the vial) indicates the physical stability of the system over time. The positive peak on the upper part of the vial in the ΔBS plot (Fig. 8B; 40—45 mm) might be caused by of a small phase separation or the presence of some bubbles.

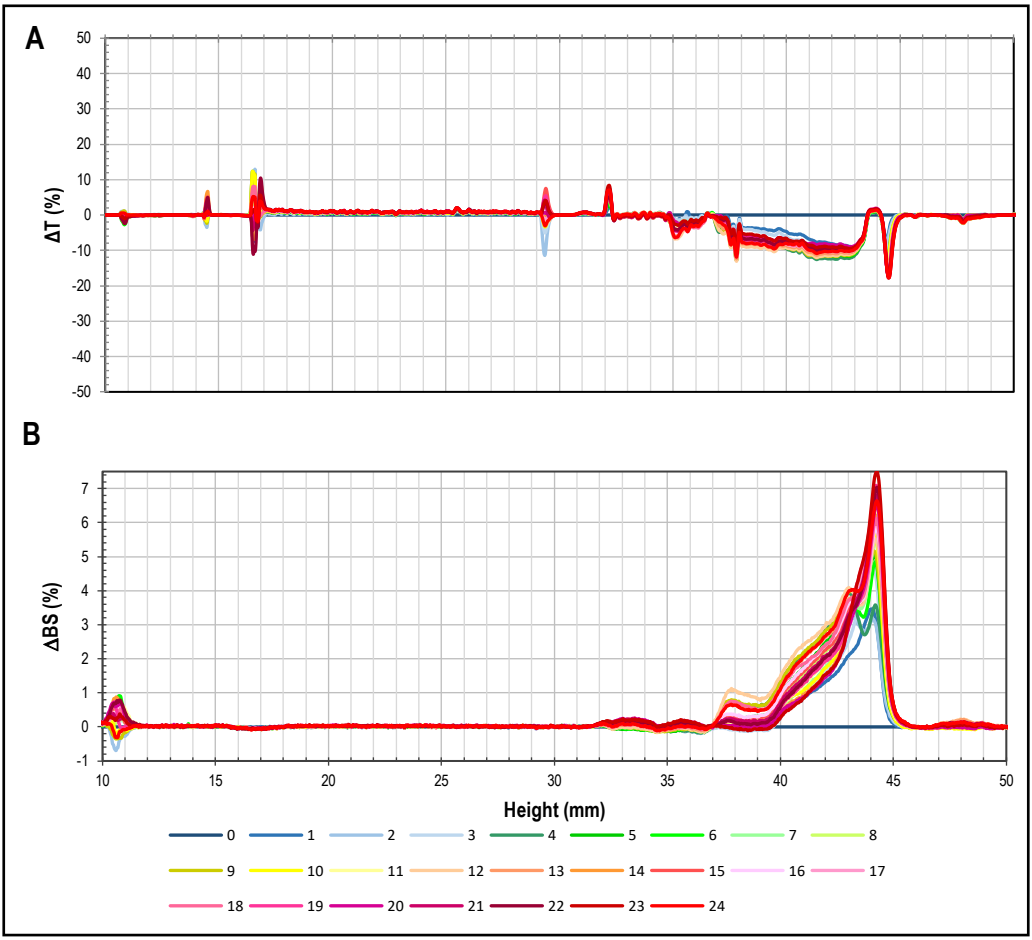

Fig. 8. A – Delta Transmission for PLGA:CH:FdU; B – Delta BackScattering for PLGA:CH:FdU.

Turbiscan stability index (TSI) shows destabilisation kinetics over time (Fig. 9). TSI >3 means important destabilization corresponding to size variation or sedimentation and creaming. TSI between 1 and 3 correspond to an initial phase of destabilisation.

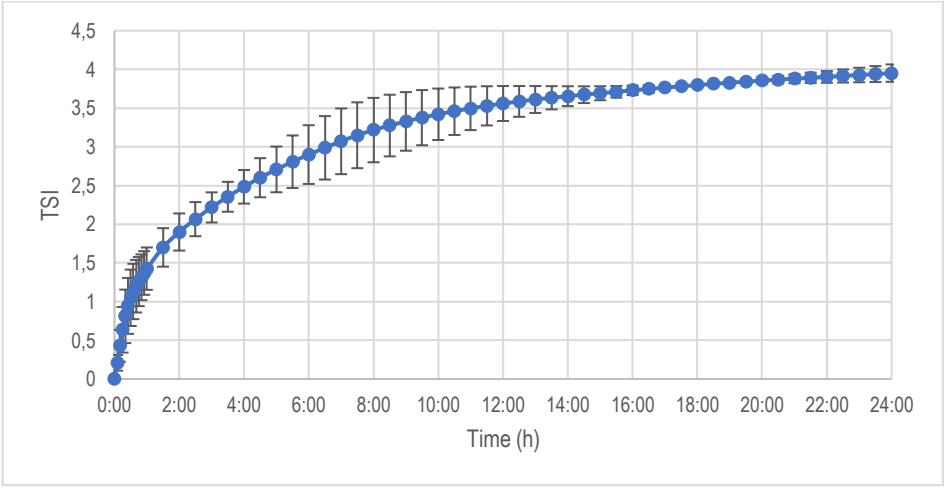

Fig. 9. Turbiscan Stability Index (TSI) for PLGA:CH:FdU.

6.1.4. Dark-Field microscopy

Dark-Field microscopy was used to confirm the encapsulation of Cou within the PLGA polymeric matrix. Figure 10A shows fluorescence of nanoparticles thus confirming encapsulation of Cou. Figure 10B and C shows nanoparticles with each component mapped in different colours, Appendix 1 shows microscopy image for each component individually.

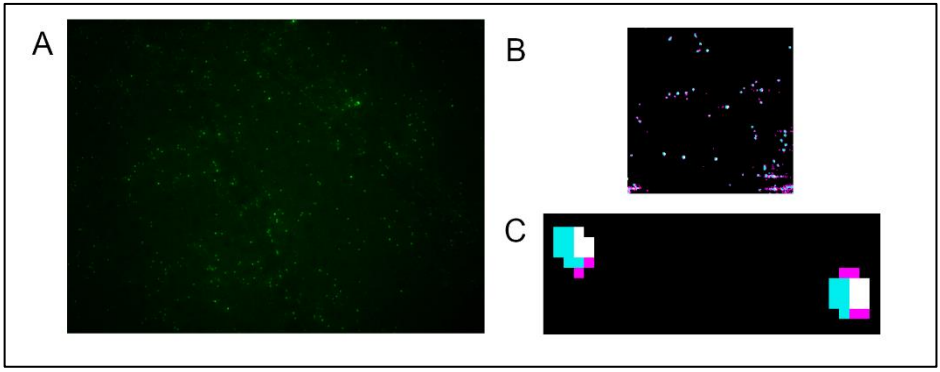

Fig. 10. A – Dark-Field microscopy fluorescence image; B – nanoparticles image; C – zoom of individual nanoparticles. PLGA mapped white, chitosan mapped cyan and FdU mapped magenta.

6.2. *IN VITRO* DRUG RELEASE OF FERULIC ACID

We did an in vitro release study of a hydrophobic substance (Coumarin-6) using the ternary system (PLGA:CH:FdU) but there was no cumulative release. Instead, FA was selected as model drug to study the release from PLGA NPs with no surface modifications. FA was encapsulated leading to corresponding FA-loaded PLGA NPs (Fig. 11). The encapsulation efficiency (%EE) of FA in PLGA was about 90%, according to data recorded in previous work at the same group. We used 1X PBS as a receptor phase and sink conditions were maintained over time. The cumulative amount of FA was monitored by HPLC at different incubation times. We observed that PLGA released the drug in a gradual and controlled way, reaching a plateau at 50% of drug released after 9 h (Fig. 11).

The release kinetics was studied using first order, Hixson-Crowell, Higuchi and Korsmeyer-Peppas equations. FA release best fitted the Korsmeyer-Peppas kinetic model ($R^2 > 0.9$) (Appendix 3). According to Peppas' equation, FA release gave an *n* (diffusion coefficient) value of 0.4256, which indicates a Fickian diffusion.

The release of not-encapsulated FA and FA-loaded PLGA NPs was studied using PBS:Ethanol (15% of Ethanol) as receptor phase for comparison purposes. FA solution reached higher values of cumulative release than encapsulated FA at the same conditions (60% of FA release versus 43% for unloaded and FA-loaded NPs, respectively). Therefore, it can be reasonably assumed that FA was encapsulated within PLGA NPs (Fig. 12). Surprisingly, 100% release of neat FA is not achieved, the cause might be interactions of hydrophobic FA with cellulose membrane of the dialysis bag. These interactions could stop FA from being released, thus explaining that only 60% of cumulative release is obtained. We found in the bibliography that also other experimentations of the release of FA did not arrive at 100% of drug released [28].

The release kinetics of FA-loaded PLGA NPs with PBS:Ethanol as receptor phase was studied with the same equations. It was found that the data best fitted the Korsmayer-Peppas kinetic model ($R^2 > 0.9$) (Appendix 3) indicating a Fickian-type diffusion (*n* value of 0.4296) same way as with FA-loaded PLGA NPs with PBS as receptor phase.

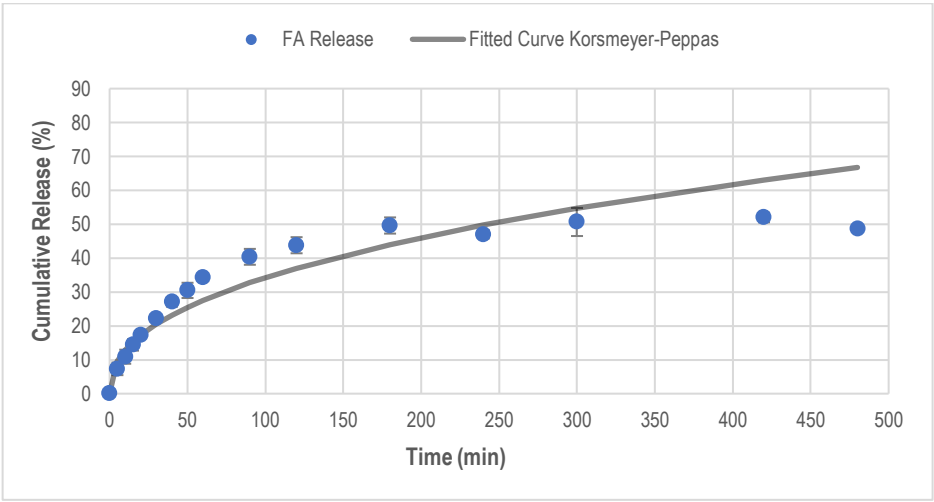

Fig. 11. Cumulative release profile of FA-loaded NPs. Receptor phase is 1XPBS.

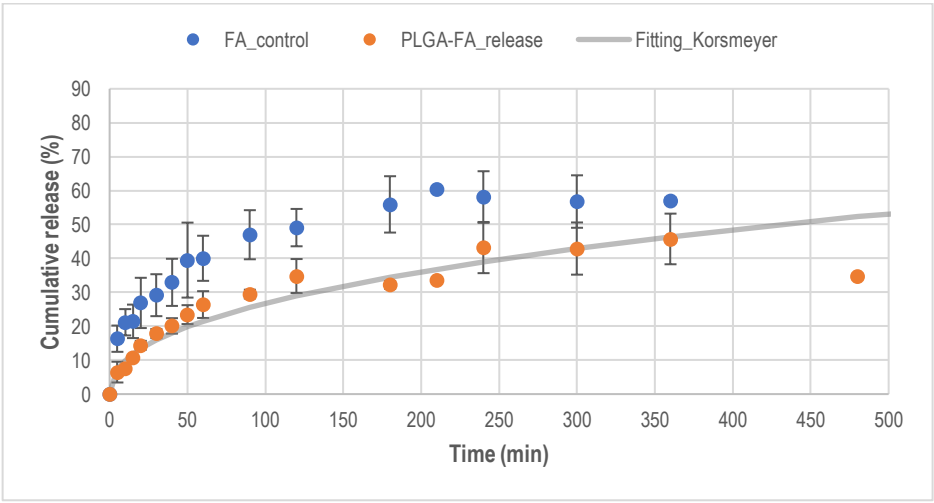

Fig. 12. Cumulative release profile of not-encapsulated FA and FA-loaded NPs. Receptor phase is PBS:Ethanol (15% ethanol).

6.3. *IN VITRO* CELL CULTURE EXPERIMENTS

6.3.1. Cellular uptake

In order to evaluate the ability of PLGA:CH system to internalise cells a flow cytometry assay was performed. As said above, for cytometry analysis Cou-loaded PLGA NPs were used, as fluorescently-labelled NPs are necessary to carry out this sort of experiment. Firstly, we selected a region (R-1) for non-treated HeLa cells (Fig. 13A) as a means to distinguish them over fluorescent labelled cells. A second region (R-2) was selected (Fig. 13B) in order to quantify the amount of positive cells that were able to incorporate Cou. Figure 13D shows the dot-lot analysis of treated HeLa cells showing that more than 90% of the cells contained the fluorescent dye. In Figure 13E, an overlay histogram of non-treated and treated cells is shown, where the shift between non-fluorescent and fluorescent-labelled cells is clearly visible.

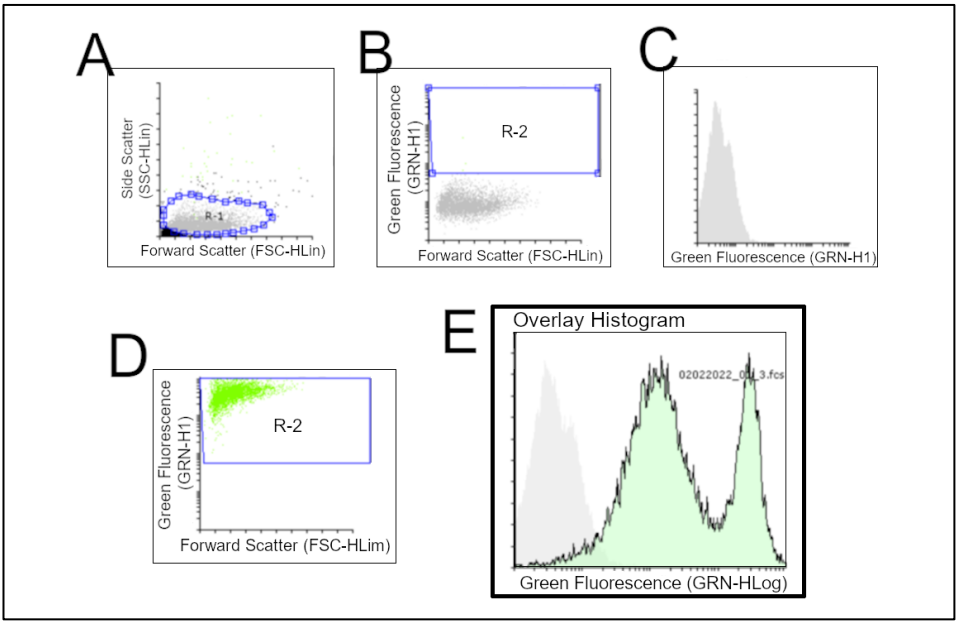

Fig. 13. Flow cytometry analysis of Cou-loaded PLGA:CH NPs in HeLa cells. A – Non-treated HeLa cells (blank); B – Control; C – Histogram of the blank; D – Treated HeLa cells; E – Overlay histogram of treated and non-treated cells.

6.3.2. MTT Assay

To assess cytotoxicity of the ternary system (molar ratio 46:2:1) a MTT assay was performed using HeLa cell lines. The range of concentrations of PLGA was 0.06 – 0.03 mg/mL (as described in Table 2) and, as controls: PLGA, PLGA:CH and FdU that were evaluated at the same conditions and concentrations of the ternary system.

Interestingly, PLGA:CH:FdU showed inhibition of cell proliferation at these low concentrations but no significative difference between the concentrations studied (68%, 69%, 68% and 69% of cell viability for 0.03, 0.04, 0.05 and 0.06 mg/mL of PLGA respectively). Interestingly, the binary system (PLGA:CH) did not affect the cellular proliferation of HeLa cells lines whereas non-complexed FdU presented values between 63 and 82%. Hence it can be supposed that FdU acts as the antitumoral agent in the ternary system (Fig. 14).

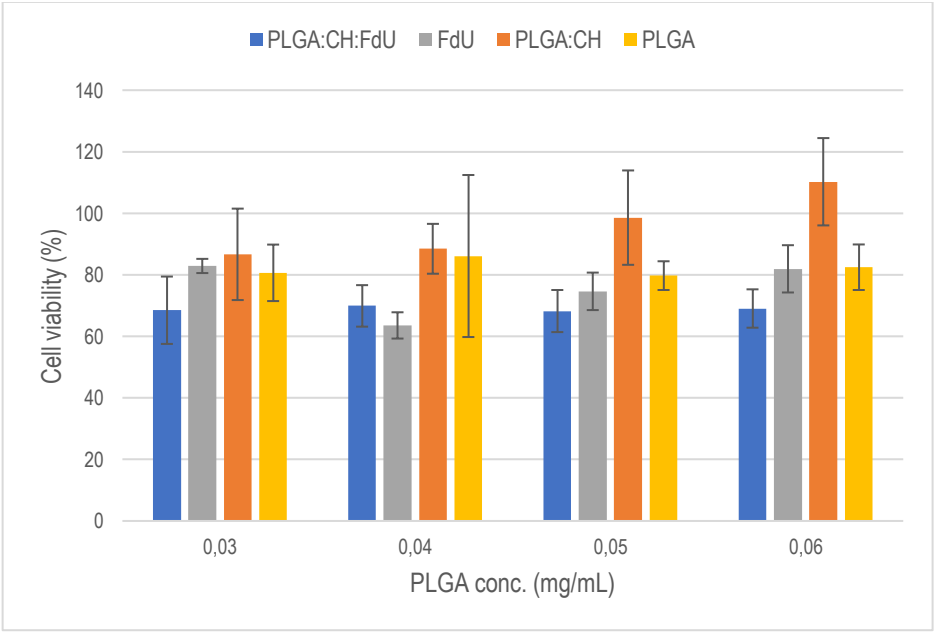

Fig. 14. Viability of HeLa cells with PLGA:CH:FdU (blue colour), FdU (grey colour), PLGA:CH (orange) and PLGA (yellow colour) at different concentrations of PLGA. FdU concentrations were $6.48x10^{-8}$ M, $8.6x10^{-8}$ M, $1.08x10^{-7}$ M and $1.30x10^{-7}$M (left to right) for both the ternary system and non-complexed FdU.

7. CONCLUSION

The ternary system PLGA:CH:FdU was successfully prepared and characterised. A preparation protocol was designed and optimised to obtain particles with a small hydrodynamic diameter (suitable to pass the BBB) and PDI under 0.5. Furthermore, dark-field microscopy showed that CH and FdU were successfully incorporated in PLGA and Cou was encapsulated.

Kinetic stability of the system employing a Turbiscan Test indicated that the system was stable for 4 hours at 37 ºC, which is around the time it takes for cells to uptake nanoparticles. Moreover, we also proved the system internalization in cells by means of a cytometry analysis, demonstrating that >90% of cells contained the fluorescent dye.

The ternary system PLGA:CH:FdU was cytotoxic against HeLa cells, and we demonstrated that FdU is the component of the nanosystem that provokes the cytotoxicity. Even so, more experimentation on the designed ternary system may be needed in order to assess cytotoxicity at different concentrations or types of cells.

Even though we did not obtain good results on the release rate using the ternary system, we think that the *in vitro* release conditions are not the same as *in vivo*. Further experimentation on different conditions may perform a better view of a dual effect (FdU plus encapsulated drug) antitumoral system.

8. REFERENCES AND NOTES

1. Herholz, K.; Langen, K.-J.; Schiepers, C.; Mountz, J. M. Brain Tumors. *Seminars in Nuclear Medicine* **2012**, *42* (6), 356–370. https://doi.org/10.1053/j.semnuclmed.2012.06.001.
2. Black, P. McL. Brain Tumors. *New England Journal of Medicine* **1991**, *324* (21), 1471–1476. https://doi.org/10.1056/NEJM199105233242105.
3. DeAngelis, L. M. Brain Tumors. *New England Journal of Medicine* **2001**, *344* (2), 114–123. https://doi.org/10.1056/NEJM200101113440207.
4. Castro, M. G.; Cowen, R.; Williamson, I. K.; David, A.; Jimenez-Dalmaroni, M. J.; Yuan, X.; Bigliari, A.; Williams, J. C.; Hu, J.; Lowenstein, P. R. Current and Future Strategies for the Treatment of Malignant Brain Tumors. *Pharmacology & Therapeutics* **2003**, *98* (1), 71–108. https://doi.org/10.1016/S0163-7258(03)00014-7.
5. Gutman, R. L.; Peacock, G.; Lu, D. R. Targeted Drug Delivery for Brain Cancer Treatment. *Journal of Controlled Release* **2000**, *65* (1–2), 31–41. https://doi.org/10.1016/S0168-3659(99)00229-1.
6. Kapoor, D. N.; Bhatia, A.; Kaur, R.; Sharma, R.; Kaur, G.; Dhawan, S. PLGA: A Unique Polymer for Drug Delivery. *Therapeutic Delivery* **2015**, *6* (1), 41–58. https://doi.org/10.4155/tde.14.91.
7. Danhier, F.; Ansorena, E.; Silva, J. M.; Coco, R.; Le Breton, A.; Préat, V. PLGA-Based Nanoparticles: An Overview of Biomedical Applications. *Journal of Controlled Release* **2012**, *161* (2), 505–522. https://doi.org/10.1016/j.jconrel.2012.01.043.
8. Levenberg, S.; Huang, N. F.; Lavik, E.; Rogers, A. B.; Itskovitz-Eldor, J.; Langer, R. Differentiation of Human Embryonic Stem Cells on Three-Dimensional Polymer Scaffolds. *Proceedings of the National Academy of Sciences* **2003**, *100* (22), 12741–12746. https://doi.org/10.1073/pnas.1735463100.
9. Tadros, T.; Izquierdo, P.; Esquena, J.; Solans, C. Formation and Stability of Nano-Emulsions. *Advances in Colloid and Interface Science* **2004**, *108–109*, 303–318. https://doi.org/10.1016/j.cis.2003.10.023.
10. Gutiérrez, J. M.; González, C.; Maestro, A.; Solè, I.; Pey, C. M.; Nolla, J. Nano-Emulsions: New Applications and Optimization of Their Preparation. *Current Opinion in Colloid & Interface Science* **2008**, *13* (4), 245–251. https://doi.org/10.1016/j.cocis.2008.01.005.
11. Taylor, P. Ostwald Ripening in Emulsions. **1998**, 57.
12. Solans, C.; Solé, I. Nano-emulsions: Formation by low-energy methods. *Current Opinion in Colloid & Interface Science* **2012**, *17*, 246–254. https://doi.org/10.1016/j.cocis.2012.07.003.
13. Solans, C.; Izquierdo, P.; Nolla, J.; Azemar, N.; Garciacelma, M. Nano-Emulsions. *Current Opinion in Colloid & Interface Science* **2005**, *10* (3–4), 102–110. https://doi.org/10.1016/j.cocis.2005.06.004.
14. Naskar, S.; Kuotsu, K.; Sharma, S. Chitosan-Based Nanoparticles as Drug Delivery Systems: A Review on Two Decades of Research. *Journal of Drug Targeting* **2019**, *27* (4), 379–393. https://doi.org/10.1080/1061186X.2018.1512112.
15. Rinaudo, M. Chitin and Chitosan: Properties and Applications. *Progress in Polymer Science* **2006**, *31* (7), 603–632. https://doi.org/10.1016/j.progpolymsci.2006.06.001.
16. Lu, B.; Lv, X.; Le, Y. Chitosan-Modified PLGA Nanoparticles for Control-Released Drug Delivery. *Polymers* **2019**, *11* (2), 304. https://doi.org/10.3390/polym11020304.
17. Chakravarthi, S. S.; Robinson, D. H. Enhanced Cellular Association of Paclitaxel Delivered in Chitosan-PLGA Particles. *International Journal of Pharmaceutics* **2011**, *409* (1–2), 111–120. https://doi.org/10.1016/j.ijpharm.2011.02.034.
18. Grem, J. L. 5-Fluorouracil: Forty-Plus and Still Ticking. A Review of Its Preclinical and Clinical Development. 16.

19. Uchikubo, Y.; Hasegawa, T.; Mitani, S.; Kim, H.-S.; Wataya, Y. Mechanisms of Cell Death Induced by 5-Fluoro-2'-Deoxyuridine (FUdR)--Necrosis or Apoptosis after Treated with FUdR--. *Nucleic Acids Symposium Series* **2002**, *2* (1), 245–246. https://doi.org/10.1093/nass/2.1.245.
20. Eidinoff, M. L.; Rich, M. A. Growth Inhibition of a Human Tumor Cell Strain by 5-Fluoro-2'-Deoxyuridine: Time Parameters for Subsequent Reversal by Thimidine. *Cancer Research* **1959**, *19*, 521–524.
21. Bhattacharjee, S. DLS and Zeta Potential – What They Are and What They Are Not? *Journal of Controlled Release* **2016**, *235*, 337–351. https://doi.org/10.1016/j.jconrel.2016.06.017.
22. Arzenšek, D. (2010, May 19) Dynamic Light Scattering and Application to Proteins in Solutions [Seminar paper]. University of Ljubljana, Lubljana.
23. Mosmann, T. Rapid Colorimetric Assay for Cellular Growth and Survival: Application to Proliferation and Cytotoxicity Assays. *Journal of Immunological Methods* **1983**, *65* (1–2), 55–63. https://doi.org/10.1016/0022-1759(83)90303-4.
24. Wang, F.; Yuan, J.; Zhang, Q.; Yang, S.; Jiang, S.; Huang, C. PTX-Loaded Three-Layer PLGA/CS/ALG Nanoparticle Based on Layer-by-Layer Method for Cancer Therapy. *Journal of Biomaterials Science, Polymer Edition* **2018**, *29* (13), 1566–1578. https://doi.org/10.1080/09205063.2018.1475941.
25. Kaur, S.; Manhas, P.; Swami, A.; Bhandari, R.; Sharma, K. K.; Jain, R.; Kumar, R.; Pandey, S. K.; Kuhad, A.; Sharma, R. K.; Wangoo, N. Bioengineered PLGA-Chitosan Nanoparticles for Brain Targeted Intranasal Delivery of Antiepileptic TRH Analogues. *Chemical Engineering Journal* **2018**, *346*, 630–639. https://doi.org/10.1016/j.cej.2018.03.176.
26. Oller-Salvia, B.; Sánchez-Navarro, M.; Giralt, E.; Teixidó, M. Blood-brain barrier shuttle peptides: an emerging paradigm for brain delivery. *Chemical Society Reviews* **2016**, *45* (17), 4631—4852. https://doi.org/10.1039/c6cs00076b.
27. Prasanna, A.; Pooja, R.; Suchithra, V.; Ravikumar, A.; Kumar Gupta, P.; Niranjan, V. Smart Drug Delivery Systems for Cancer Treatment Using Nanomaterials. *Materials Today: Proceedings* **2018**, *5* (10), 21047—21054. https://doi.org/10.1016/j.matpr.2018.06.498.
28. Saini, S.; Sharma, T.; Jain, A.; Kaur, H.; Katare, O.P.; Singh, B. Systematically designed chitosan-coated solid lipid nanoparticles of ferulic acid for effective management of Alzheimer's disease: A preclinical evidence. *Colloids and Surfaces B: Biointerfaces* **2021**, *205*, 111838. https://doi.org/10.1016/j.colsurfb.2021.111838.

9. ACRONYMS

BBB: Blood-brain barrier

CH: Chitosan

CNS: Central Nervous System

Cou: Coumarin-6

DLS: Dynamic Light Scattering

FA: *trans*-Ferulic acid

FdU: 5-fluorodeoxyuridine

NPs: Nanoparticles

PLGA: Poly(lactic-co-glycolic acid)

APPENDICES

APPENDIX 1: DARK-FIELD MICROSCOPY INDIVIDUAL IMAGES

Individual images of Dark-Field microscopy for each component are reported here.

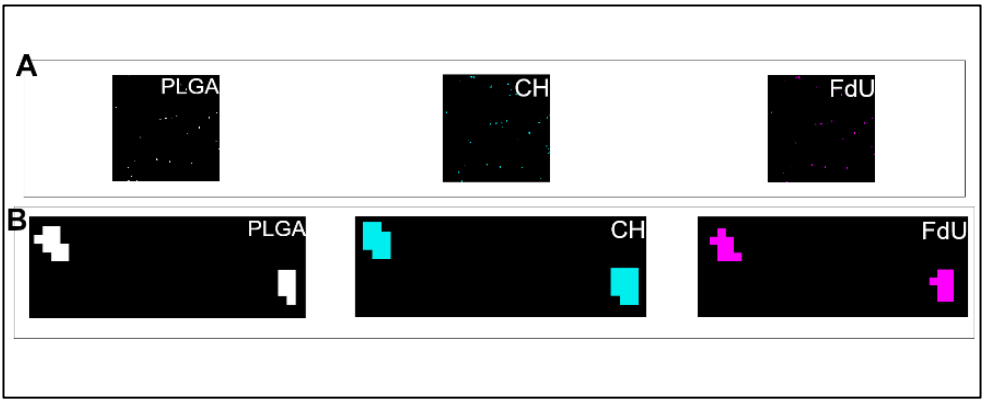

Fig. 15. Dark-Field microscopy images. A – Mapping of the individual components of the ternary System; B – Zoom of individual particles for each component.

APPENDIX 2: CALIBRATION CURVE OF FERULIC ACID

A calibration curve was needed in order to perform the release of Ferulic Acid. Stock solutions of known concentrations were measured by HPLC with an UV lamp utilizing ACN/H_2O as mobile phase.

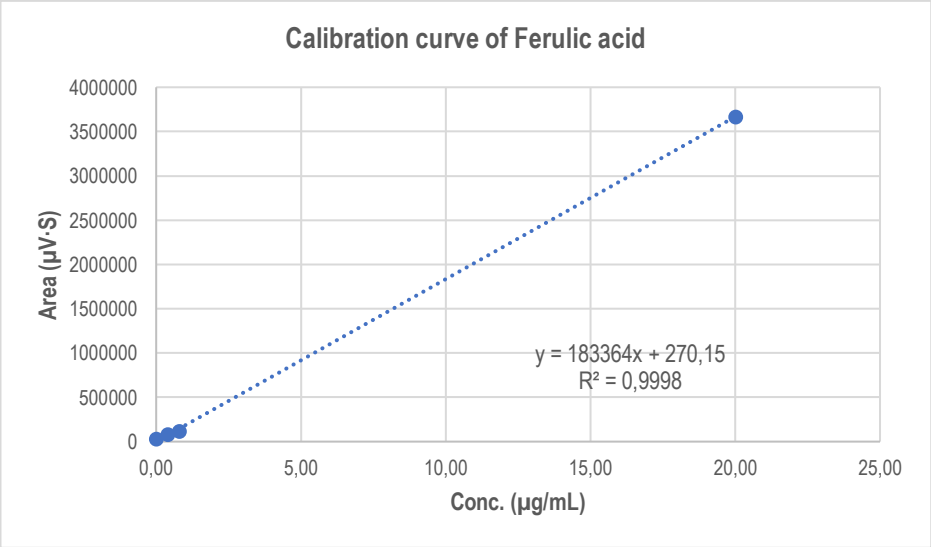

Fig. 16. Calibration curve of Ferulic acid.

APPENDIX 3: FA RELEASE KINETIC MODEL

Figures 17 and 18 shows that FA release (both in PBS and PBS:Ethanol as receptor phase) follows a Korsmeyer-Peppas kinetic model considering that it is the model with a regression coefficient closest to 1 ($R^2 > 0.9$).

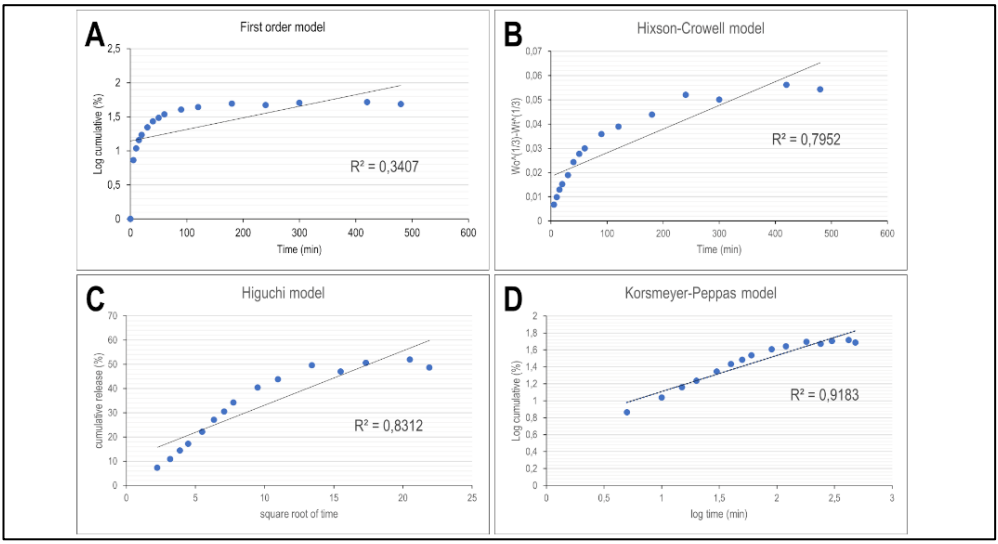

Fig. 17. Mathematical models for FA release with PBS as receptor phase. A- First order model; B – Hixson-Crowell Model; C – Higuchi model; D – Korsmeyer-Peppas model.

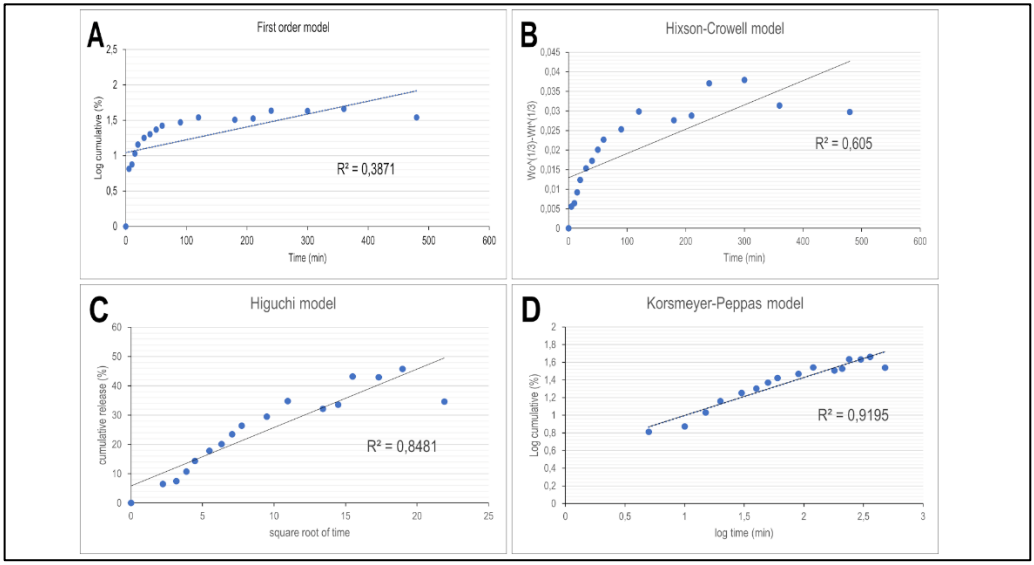

Fig. 18. Mathematical models studied of FA release with PBS:Ethanol as receptor phase. A- First order model; B – Hixson-Crowell Model; C – Higuchi model; D – Korsmeyer-Peppas model.